Hydro-morphological modelling of small, wave-dominated estuaries

Slinger, Jill H.

DOI
10.1016/j.ecss.2016.10.038

Publication date
2016

Document Version
Proof

Published in
Estuarine, Coastal and Shelf Science

Estuarine, Coastal and Shelf Science xxx (2016) 1–14

Contents lists available at ScienceDirect

Estuarine, Coastal and Shelf Science

journal homepage: www.elsevier.com/locate/ecss

Hydro-morphological modelling of small, wave-dominated estuaries

Jill H. Slinger [a, b, *]

[a] Delft University of Technology, Jaffalaan 5, 2628 BX Delft, The Netherlands
[b] Institute for Water Resources, Rhodes University, Old Geology Building, Artillery Road, Grahamstown, 6140, South Africa

ARTICLE INFO

Article history:
Received 8 March 2016
Received in revised form
14 October 2016
Accepted 30 October 2016
Available online xxx

Keywords:
Intermittently open estuary
Episodic closure
Parametric modelling
Bar-built
Tidal inlet
Freshwater flows
Climate change
South Africa

ABSTRACT

Small, intermittently open or closed estuaries are characteristic of the coasts of South Africa, Australia, California, Mexico and many other areas of the world. However, modelling attention has tended to focus on big estuaries that drain large catchments and serve a wide diversity of interests e.g. agriculture, urban settlement, recreation, commercial fishing. In this study, the development of a simple, parametric, system dynamics model to simulate the opening and closure of the mouths of small, wave-dominated estuaries is reported. In the model, the estuary is conceived as a basin with a specific water volume to water level relationship, connected to the sea by a channel of fixed width, but variable sill height. Changes in the form of the basin are not treated in the model, while the dynamics of the mouth channel are central to the model. The magnitude and direction of the flow through the mouth determines whether erosion or deposition of sediment occurs in the mouth channel, influencing the sill height. The model is implemented on the Great Brak Estuary in South Africa and simulations reveal that the raised low water levels in the estuary during spring tide relative to neap tide, are occasioned by the constriction of the tidal flow through the shallow mouth. Freshwater inflows to the estuary are shown to be significant in determining the behaviour of the inlet mouth, a factor often ignored in studies on tidal inlets. Further it is the balance between freshwater inflows and wave events that determines the opening or closure of the mouth of a particular estuary.

1. Introduction

Intermittently open or closed estuaries characterize the coasts of South Africa, Australia, west Africa, California, Mexico and many other areas of the world (Cooper, 2001; Taljaard et al., 2009; Roy et al., 2001; Ranasinghe et al., 1999; Ranasinghe and Pattiaratchi, 2003; Goodman, 1996; Anthony et al., 2002; Jacobs et al., 2011; McLaughlin et al., 2013; Mendoza et al., 2009). These wave-dominated estuaries tend to be small in comparison with river- or tidally-dominated systems (Dalrymple et al., 1992), and the inlet mouths are highly dynamic. Modelling attention has focused on larger estuaries, serving many powerful sectoral interests such as navigation, agriculture, urban settlement, commercial fishing, recreation and tourism. Existing 2-D and 3-D process-based models represent the circulation and sedimentation in large estuaries reliably (e.g. Lesser et al., 2004), but have difficulty in accurately simulating the complex processes involved in the closure and opening of inlet mouths. Recent research has focussed on improving the prediction of sedimentation near the inlet mouths with success (Elias, 2006; Tung et al., 2009; Duonga et al., 2015; Wijnberg et al., 2015). Indeed, an innovative approach using a process-based model in combination with measured data to generate a reliable and complete data set on the morphological development of a tidal inlet was developed in Portugal (Fortunatoa et al., 2014). Unfortunately, these applications require detailed data on sedimentation, are computationally intensive, and were primarily applied to large estuaries.

Two alternative approaches have recently been developed and applied to small Californian estuaries. These include the hydrologic and geomorphic approach of Rich and Keller (2013) in which the outflow over the beach of a bar-built estuary is successfully simulated. Here the emphasis lies on the influence of river inflow and groundwater on the volume flows and the influence of changing channel location and morphometry remains problematic. The data requirements for this approach are considerably reduced from those of process-based models. This is also an advantage of the parametric approach of Behrens et al. (2013, 2015), applied and calibrated on the Russian River. The approach used by Behrens et al.

* Corresponding author. Delft University of Technology, Jaffalaan 5, 2628 BX Delft, The Netherlands.
E-mail address: j.h.slinger@tudelft.nl.

http://dx.doi.org/10.1016/j.ecss.2016.10.038

(2013) is similar to that adopted in this paper, as originally developed and applied to South African estuaries (Slinger, 1996). The differences lie primarily in the manner in which the (maximal) volumetric flow through the channel is determined, and the sedimentation formulae that are applied.

Another parametric modelling approach focusing on sedimentation in a channel has been followed by Eysink and Vermaas (1983) and van Rijn (2013), who developed an empirically-based prediction tool *Sedpit* often used in conjunction with a harbour siltation model to determine dredging requirements for harbours. Recently, this model was applied to simulate sedimentation at Ijmuiden in the Netherlands with success (van Leeuwen, 2015). However, the application of such a model requires information on wave-current interactions in the nearshore zone, data on longshore sediment transport, and data on different sediment fractions for accurate application. Moreover, both the computationally intensive process-based models such as Delft3D (Lesser et al., 2004) and the empirical model *Sedpit,* have difficulty with accommodating the complexity of the dynamic processes in an inlet mouth, and frequently neglect the effect of freshwater inflows.

In this study, we address these limiting conditions, by developing a simple, parametric, system dynamics model to simulate the opening and closure of the mouths of small, wave-dominated estuaries. In the model, the estuary is conceived as a basin with a specific water volume to water level relationship, connected to the sea by a channel of fixed width, but variable sill height. Changes in the form of the basin are not treated in the model, while the dynamics of the mouth channel are central to the model. As in the approaches of Eysink and Vermaas (1983), van Rijn (2013) and Behrens et al. (2013, 2015), the magnitude and direction of the flow through the mouth determines whether erosion or deposition of sediment occurs in the mouth channel. Erosion reduces the sill height, while deposition increases the sill height. We then illustrate the application of the model with a detailed case: the Great Brak Estuary in South Africa, a small, intermittently closed system typical of many estuaries along the South African coast. Data on both the opening and closure of the estuary mouth and the associated circulation in the estuary are available from a number of measurement campaigns. Whereas an Escoffier analysis (cf. Goodman, 1996) simply places the case study estuary into the unstable, or even the normally closed, category, we are able to establish that the estuary suffers an increase in the frequency and persistence of mouth closure owing to reductions in freshwater inflows.

The model further sheds light on the primary determinant of the higher low water levels during spring tide than during neap tide in small, wave-dominated estuaries, and confirms that the balance between freshwater inflows and wave events plays a significant role in mouth opening or closure.

First, the formulation of the model is described with reference to the relevant literature in section 2. Then, the choice for simulation method and a description of the case study are provided in the first part of section 3. Next, the application to the case is explained in the rest of section 3. This is followed by a discussion and conclusion in sections 4 and 5, respectively.

2. Model formulation

The estuary is conceived as a basin with a specific hypsometry, connected to the sea by a channel of fixed width, but variable sill

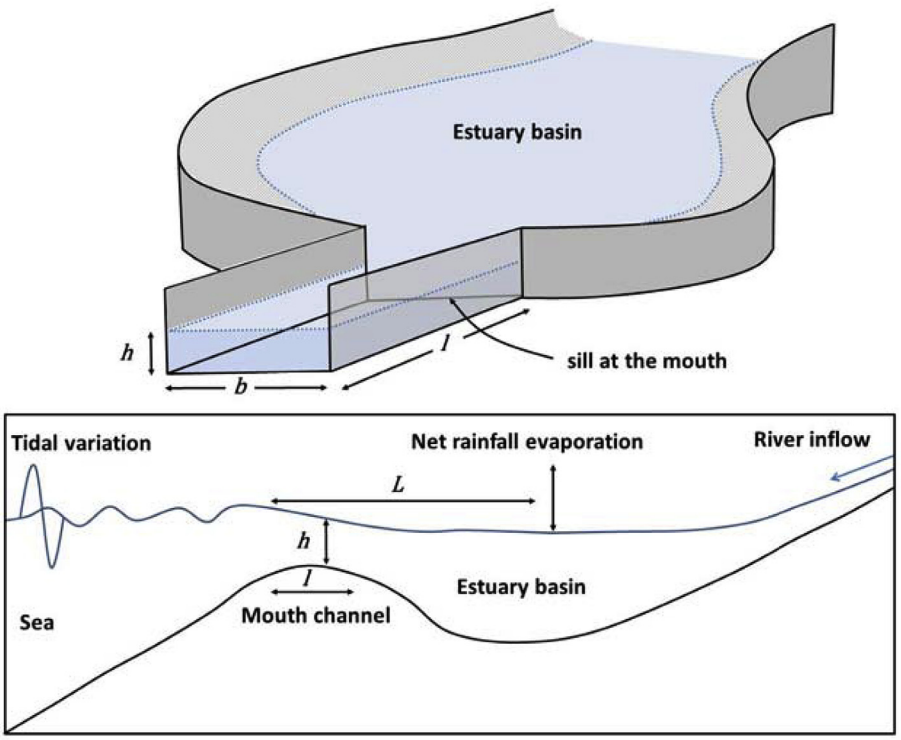

Fig. 1. The mouth is modelled as a rectangular channel connected to an estuary basin at the sill height. The dimensions of the mouth are depicted frontally above (adapted from Slinger 1996), and in side view below. The effective depth of flow (h), the width of the mouth (b), the length of the mouth (l) and the characteristic length scale (L), are indicated.

Please cite this article in press as: Slinger, J.H., Hydro-morphological modelling of small, wave-dominated estuaries, Estuarine, Coastal and Shelf Science (2016), http://dx.doi.org/10.1016/j.ecss.2016.10.038

height (Fig. 1). Changes in the form of the basin are not treated in the model, while the dynamics of the mouth channel are central to the model. The model therefore comprises two sectors. The first deals with factors affecting the water volume in the estuary: water volume sector. The second covers the dynamics of the sill height at the mouth of the estuary: sediment sector. A full listing of the model equations and parameter names can be found in Tables A1 and A2 in the Appendix.

2.1. Water volume sector

The volume of water in the estuary (x_1) is determined by four rates: the freshwater inflow rate (x_{11}), the net precipitation evaporation rate(x_{12}), the seepage rate (x_{13}), and the tidal flow through the mouth (x_{14}). The riverine inflow to the estuary increases the water volume, while the net precipitation evaporation usually acts to increase the water volume apart from during hot spells. The seepage rate is included to either reflect the loss of water from the estuary through the sand bar at the mouth, or the presence of freshwater seeps in the middle and upper reaches of the estuary. However, it is the tidal flux through the estuary mouth that is of primary interest for the dynamics of a small estuary.

The direction of the tidal flux through the mouth depends on whether the tidal water level in the sea exceeds the water level in the estuary or *vice versa*. The effects of wave set-up in elevating the water level in the sea are not taken into account. When the water level within the estuary exceeds the tidal water level in the sea (and the sill height), water flows from the estuary into the sea constituting the ebb tide. Similarly, when the tidal water level exceeds both the water level within the estuary, and the sill height, sea water flows into the estuary, forming the flood tide. The tidal flow rates through the mouth are formulated as directly proportional to the head difference (h_L), that is the difference between the tidal water level (*twl*) and the water level in the estuary (*wl*). However, for a given head difference ($h_L = twl - wl$), the flow through the mouth will differ according to (i) the form of the estuary basin, (ii) the effects of bottom friction, and (iii) the effect of the estuary mouth.

(i) The form of the estuary basin

The effects of the estuary basin are taken into account in the model by introducing a characteristic length parameter (L) over which the hydraulic head is assumed to act (Fig. 1), and by including a hypsometric curve that relates water levels to water volumes ($H_s'(wl)$). L is determined as the distance from the mouth to the point in the small, wave-dominated estuary basin where water level variations are most representative of the estuary dynamics. This allows the differentiation of different estuary shapes. For instance if two estuaries with the same water level to water volume relationship, the same hypsometric curve, have different characteristic lengths, we know that the estuary with the greater characteristic length has a longer and narrower form than the shorter, broader estuary with the lower characteristic length.

(ii) The effects of bottom friction

Friction is important in all estuarine systems and dominant in shallow estuaries (Green, 1837; Ippen and Harleman, 1966), but bottom friction effects are significant in small, shallow estuaries with narrow, constricted mouths and well developed flood tidal deltas (Aubrey and Speer, 1985; Speer and Aubrey, 1985). Distortion in tidal fluxes and velocity asymmetries result (Lincoln and FitzGerald, 1988; Morris and Turner, 2010). The highest current velocities through the mouth in wave-dominated estuaries occur during the shorter, more intense flood component of the tidal cycle. The current velocities during ebb tend to be lower, but persist for longer over the longer ebb component of the tidal cycle. In South African estuaries the ebb tide may persist twice as long as the flood tide (i.e. lasting approximately 8 h, while the flood tide lasts only a little over 4 h (cf. Slinger et al., 1994)). The non-linear differences between the ebb and flood tidal velocities for a given head difference are incorporated in the model via a velocity asymmetry function (V(twl,wl)). The shape of this function may be determined from measurements of flood and ebb flow velocities within the basin of a particular estuary, near the mouth (cf. Lincoln and FitzGerald, 1988; Morris and Turner, 2010).

(iii) The effect of the estuary mouth

The effects of the form of the estuary basin and bottom friction on the tidal flux through the mouth are not of such severity as to prevent tidal exchange. In contrast, the mouth of an estuary may be closed or so constricted that tidal exchange is curtailed. The influence of mouth configuration on tidal exchange is modelled by first considering the exchange that would occur without this constraining influence – the target tidal flux (*ttflux*) – and then determining the magnitude of the reduction owing to mouth constriction.

$$ttflux = \frac{h_L}{L} H_s'(wl) V(twl, wl) \tag{1}$$

In a given time period the target tidal flux (1) may not be able to enter or exit the estuary because of the constriction or closure of the mouth. Indeed, Officer (1976) demonstrated that for steady one layer flow (given energy) a shallowing or constriction in a channel exercises a limiting effect on the flow volume with the maximum flow condition proving to be the critical flow condition. Importantly, the shallowing (decrease in depth) and/or contraction (decrease in width) of an estuary mouth was demonstrated to exercise internal hydraulic control on two-layer exchange flow through the mouth (Stommel and Farmer, 1953; Farmer and Armi, 1986; Armi and Farmer, 1986). Such two-layer exchange flow and associated two-layer flow was observed to occur in the Palmiet Estuary in South Africa (Largier and Slinger, 1991), and the occurrence of features associated with such control (e.g. tidal intrusion fronts) in other small estuaries is confirmed by Schumann et al. (1999). This means that, in contrast to tidally dominated estuaries, a (maximal) critical flow volume can be associated with tidal exchange at the mouth of small, wave-dominated estuaries as explained hereafter, to include this constraining effect of the mouth on tidal volume exchange, we first calculate the cross-sectional area of the mouth at a particular time, and then determine the critical flow volume.

The estuary mouth is conceptualized as a channel of fixed width, but variable sill height connected to the estuary basin (Fig. 1a), so the mouth cross-sectional area (a) through which tidal flow may occur, is calculated as the product of the width (b) and the effective depth of flow (h). The effective depth of flow (2) is given by the difference between the greater of the tidal water level or the water level in the estuary, and the height of the sill at the mouth (x_2). When the height of the sill exceeds the water levels of both the sea and the estuary, the effective depth of flow is zero, the mouth is closed ($a = bh = 0$) and the tidal flux is zero.

Please cite this article in press as: Slinger, J.H., Hydro-morphological modelling of small, wave-dominated estuaries, Estuarine, Coastal and Shelf Science (2016), http://dx.doi.org/10.1016/j.ecss.2016.10.038

$$h = \begin{cases} twl - x_2 & \text{if } twl > wl \text{ and } twl > x_2 \\ wl - x_2 & \text{if } wl \geq twl \text{ and } wl > x_2 \\ 0 & \text{otherwise} \end{cases} \quad (2)$$

For a fluid flowing through a channel constriction or shoal, the critical flow velocity is the velocity at which the Froude number is unity (Officer, 1976). However, in the region of an estuary mouth, where single- or two-layer flow characteristically occurs, the exchange of fluids with different densities takes place. The critical flow condition then occurs when the two-layer composite Froude number, defined as $G^2 = F_1^2 + F_2^2$, is unity; where $F_i^2 = u_i / \sqrt[2]{g' h_i}$ and F_i is the layer densimetric Froude number, u_i is the layer fluid velocity, g' is reduced gravitational acceleration, and h_i is layer depth (Largier and Slinger, 1991). However, the *net volume flow is maximum* when the critical condition for uni-directional flow applies either at the seaward or landward side of the mouth. This occurs, for instance, on the landward side of the mouth if the mouth channel is filled with seawater pushing into the estuary on the flood tide, and it occurs on the seaward side of the mouth if the mouth channel is filled with estuarine water draining from the estuary on the ebb tide. This critical condition occurs when the densimetric Froude number for the active layer is unity, that is $u_i = \sqrt[2]{g' h_i}$ where layer i (seawater or estuarine water) is flowing actively. It is this condition that we use in determining a maximal volume flux (an upper limit) that can flow through the mouth. Because $g' < g$, the critical layer velocity for uni-directional flow over depth h is less when density differences are present than when they are absent. A density difference of 6–15 kg m^3 between the seawater entering the estuary at the height of the flood tide and the ambient estuary water may be assumed for a number of South African estuaries (Slinger et al., 1994; Taljaard et al., 2009). Then, using the effective depth of flow in the mouth (h), we can calculate a critical flow velocity, which together with the mouth cross-sectional area (a), allows us to establish dynamically an *upper limit for the maximum critical flow volume*. The actual volume flux through the mouth is likely to be less than the maximum critical flow volume most of the time. Therefore, if the target tidal flux is less than a critical flow volume $u_c a = \sqrt[2]{gh}.a$ (with g used instead of g' to yield the upper limit), no reduction of the target tidal flux occurs, and the mouth has no constraining effect on the tidal flow. However, if the target tidal flux exceeds the critical flow volume, the target tidal flux is then constrained by multiplying it by the control factor (c_f), which then has a value less than unity (3,4).

$$c_f = \begin{cases} \dfrac{u_c a}{|ttflux|} & \text{if } u_c a < |ttflux| \\ 1 & \text{otherwise} \end{cases} \quad (3)$$

$$x_{14} = ttflux.c_f \quad (4)$$

In conclusion, the intra-tidal momentum effect, which is a term describing the delay in the transition from ebb to flood tide and *vice versa* (slack water) over the estuary as a whole, is not included explicitly in the tidal flux formulation as this would require the simulation of variations in water level along the length of the estuary. Given that we are explicitly modelling small estuaries, the omission of the momentum condition and the concomitant ability to simulate changes in the state of the mouth in response to different wave and freshwater inflow conditions over longer time periods, following the careful specification of model parameters, seems an acceptable trade-off. The water volume in the estuary is given by differential equation (A.1), completing the formulation of the water volume sector.

$$\frac{dx_1}{dt} = \sum_{i=1}^{4} x_{1i} \quad (A.1)$$

2.2. Sediment sector

The sediment responsible for the constriction or closure of a bar-built, wave-dominated estuary mouth derives primarily from the marine environment (Morris and Turner, 2010). The mouth clogs with marine sand rather than the finer terrigenous material found in the upper and middle reaches. Accordingly, the erosion or accretion of the sandy sill at the mouth of the estuary, as well as artificial breaching, are the only aspects of estuary morphodynamics included in the sediment sector. The sill height (x_2) is determined by three rates: the erosion rate (x_{21}), the accretion rate (x_{22}), and the breaching rate (x_{23}). Whereas the erosion rate and the accretion rate are calculated endogenously, the breaching rate is an input (policy) parameter in the model.

The sediment accreting or eroding in the mouth inlet is transported by the tidal flux, either as bed load or in the water column. There are many formulae for sediment transport, each more or less accurate depending on the particular application (Nakato, 1990; van Rijn, 2013). Because the mouth is assumed as a rectangular channel experiencing net uni-directional, non-oscillatory flow during each of the ebb and flow tides, the Ackers-White sediment transport formula (Ackers and White, 1975) is adopted. An advantage of this formula is that it deals with the total sediment load and does not consider the bed and suspended load separately. Physical considerations and dimensional analysis were used in determining the form of the Ackers-White formula, but the coefficients (original and updated) were determined using empirical data. The formula is more commonly applied to rivers, but was found to be more accurate than other transport formulae in early applications on other South African estuaries (cf. CSIR, 1991). Its success in predicting observed mouth opening and closure events with limited calibration (Slinger, 1996; this paper) mean that it has been retained in the formulation of the sediment sector of the model.

The well documented procedure for calculating the Ackers-White equation begins with the determination of the dimensionless sediment parameter $d_{gr} = d[g(s-1)/\nu^2]^{1/3}$ where d is the grain diameter, g is the gravitational acceleration, s is the specific gravity of the sediment, ν is the kinematic viscosity of water. Next a number of empirical parameters are calculated, namely the transition exponent, n, the coefficient and exponent in the sediment transport function (c and m respectively), and the initial motion parameter, S_i. For $1 \leq d_{gr} \leq 60$ the values of all of these parameters depend on the value of the dimensionless sediment parameter.

Then, Ackers and White define the particle mobility (S_{gr}) as a measure of the capacity of the flow to transport the sediment. When the particle mobility exceeds the initial motion parameter ($S_{gr} > S_i$), the critical threshold, the transport of sediment by the flow can occur. The particle mobility in turn depends upon the shear stress (u_*), and is further influenced by the mean flow ($\overline{u}$) and the depth of flow in the mouth. As the particle mobility increases above the threshold value, the capacity of the flow to transport sediment (S_t) increases according to a power relation utilizing the exponents n and m (Appendix A). Finally, the volumetric sediment transport rate, the volume of sediment that can be transported per unit volume of water) is given by $S_{vol} = S_t(d/h)(\overline{u}/u_*)^n$ where in our case $u_* = \sqrt[2]{gh|twl - wl|/l}$ and the mean flow is $\overline{u} = |x_{14}|/a\varepsilon$, where a is the mouth cross-sectional area and ε is a factor converting units

Please cite this article in press as: Slinger, J.H., Hydro-morphological modelling of small, wave-dominated estuaries, Estuarine, Coastal and Shelf Science (2016), http://dx.doi.org/10.1016/j.ecss.2016.10.038

from years to seconds. Note that the shear stress relevant to sedimentation in the mouth is calculated over the length of the mouth channel, whereas the head difference determining the flux through the mouth is determined using the characteristic length of the estuary.

For the outflowing ebb tide, a volumetric sediment transport rate can be derived based on the characteristics of the ebb tidal flow through the mouth inlet and the sediment grain size in the entrance channel. However, the configuration of the channel, parametrized as having a fixed width (b) and length (l), and the porosity of the sandy bed (p_s) of the inlet have to be taken into account before the erosion rate of the sand sill can be determined. Erosion is assumed to occur uniformly across the bed of the channel at the mouth and there is no limit to the availability of sand for erosion. Therefore, the erosion rate of the sill is given by:

$$x_{21} = \begin{matrix} S_{vol}x_{14}/bl(1-p_s) & \text{if } x_{14} < 0 \\ 0 & \text{otherwise} \end{matrix} \quad (5)$$

In contrast to the erosion occurring on the ebb tide, the flood tidal flux is responsible for the import of sediment into the mouth channel. Indeed, the presence of waves is known to increase the concentration of sediment in suspension (Nadaoka et al., 1988; van Rijn, 2007; Héquettea et al., 2008) and to cause elevated concentrations to be transported into the entrance channel where constriction and shallowing cause a sharp reduction in wave activity (Day, 1981). Enhanced deposition of sediment results, clogging the mouth and forming the flood tidal delta immediately landward of the constricted inlet (Morris and Turner, 2010). These effects cannot be ignored. A standard application of the Ackers-White sediment transport formula as applied to the ebb tidal flow is therefore not appropriate. Instead, the effects of wave stirring (ω) in increasing the sediment transport capacity of the inflowing tide must be accommodated (van Rijn, 2007). It is this additional sediment that is deposited in the mouth channel clogging it and causing it to close at times, while the remaining sediment is considered to be transported beyond the mouth and into the body of the estuary. As we are not studying changes in the form of the estuary basin apart from the mouth channel, this sediment is not our focus. The applicability of the model is limited to systems where this sediment volume is insufficient to significantly alter the basin hypsometry.

Furthermore the cross-shore profile, including the beach slope, can influence the local availability of sediment immediately seaward of the mouth channel (Behrens et al., 2015). Much process-based modelling activity is devoted to an accurate determination of sediment transport under waves and currents, and varying cross-shore configurations, longshore drift conditions, and beach steepness. Here, however, the local, shoreface topographical effects are simply included in a parameter β. This parameter is set equal to unity unless there are factors such as wave sheltering or a steep beach e.g. the Mgeni Estary in South Africa, causing the enhanced suspension of sediment immediately off the estuary mouth. The wave stirring parameter ω, is an exogenously defined variable that allows the specification of a wave climate function and a wave height factor for the testing of the effects of high wave events. It may be derived from measurements of seasonal variation of the significant wave height in the nearshore zone.

The quantity of sediment transported by the combined effect of the flood tidal currents and waves into the mouth of the estuary is then determined by the Ackers-White transport formula with the sediment mobility increased by multiplying by the wave stirring and the local, shoreface topography factors (6) (cf. Behrens et al., 2015). The quantity of sediment deposited in the channel is then calculated as the difference between the quantity that would have been transported under the action of the flood tidal current alone (i.e the standard transport formula) and the quantity transported under the enhanced sediment mobility associated with a combined wave and current regime and local shoreface topography (i.e. the modified transport formula) (7). Taking into account the rectangular form of the channel (parametrized as having a fixed width (b) and length (l)) and the porosity of the deposited sandy layer, we can determine the accretion rate of the sill (8).

$$S_w = \begin{matrix} c(\omega\beta S_{gr}/S_i - 1)^m & \text{if } \omega\beta S_{gr} > S_i \\ 0 & \text{otherwise} \end{matrix} \quad (6)$$

$$S_{mod} = S_w(d/h)(\overline{u}/u_*)^n \quad (7)$$

$$x_{22} = \begin{matrix} (S_{mod} - S_{vol})x_{14}/bl(1-p_s) & \text{if } x_{14} > 0 \\ 0 & \text{otherwise} \end{matrix} \quad (8)$$

Erosion acts to decrease the sill height, while accretion increases the sill height. The mouth closes at a particular instance of time when the volume of sediment deposited in the mouth is sufficient to cause the sill height to exceed either the water level in the estuary or the tidal water level at the next instance in time. This can occur because the tide in the sea is falling or because seepage from the estuary and net precipitation-evaporation are just sufficient under low freshwater inflow conditions to cause the estuary water level to fall below the sill height. Then the sill height exceeds the greater of the tidal water level or the water level in the estuary, the effective depth of flow becomes zero, and the mouth is closed. The marine influence on the estuary water body is curtailed until the mouth is breached.

Artificial breaching of the mouth is included in the model as the exogenously specified breaching rate (x_{23}). Natural breaching of the mouth is initiated when fresh water inflows cause the water level in the estuary to increase and overtopping and scouring of the mouth by the outflowing volume of water occurs (i.e. via x_{21} not x_{23}). However, in our model, flows can never be supercritical, so the natural breaching cannot be represented fully. The rate at which natural breaching occurs in the model must necessarily be slower than in reality, and the erosion of the sill less effective. However, even with these limitations, the sill height can erode to decrease below the estuarine or tidal water level allowing the effective depth of flow to become positive - the mouth is open to tidal exchange. The sill height in the estuary is determined by differential equation (A.2), completing the formulation of the sediment sector.

$$\frac{dx_2}{dt} = \sum_{i=1}^{3} x_{2i} \quad (A.2)$$

3. Application to the Great Brak estuary, South Africa

The equations of the model were formulated using the system dynamics modelling method (Forrester, 1961, 2007; Slinger, 1996). The resulting parametric model is simple, using a hypsometric curve to parametrize the water level to volume relationship of the estuary basin, and comprising only two differential equations.

The model applied to the Great Brak Estuary is coded in Fortran and simulated using a double precision variable step numerical method with error bound set to 0,01%. Results have been compared with routines from the IMSL Fortran Numerical Library and found to agree within the error bound when applied to both

Please cite this article in press as: Slinger, J.H., Hydro-morphological modelling of small, wave-dominated estuaries, Estuarine, Coastal and Shelf Science (2016), http://dx.doi.org/10.1016/j.ecss.2016.10.038

the Great Brak and Kromme Estuaries in South Africa (Slinger, 1996). A later version of the model is coded in Vensim DSS (www.vensim.org) and simulated with a time step of 12,5 min to achieve the same level of numerical accuracy when applied to the Slufter, a small estuary in the Netherlands (D'Hont, 2014; D'Hont et al., 2014).

3.1. Case study site description

In South Africa, the 7 km Great Brak Estuary has long been a focus of attention (Slinger et al., 1994, 2005, 2012) as there are pressing management issues related to the inlet mouth. The choking of the mouth by sand deposition and the (potential) cessation of tidal exchange for prolonged periods form an ongoing problem in the sustainable management of the Great Brak Estuary (Fig. 2). After all, the character and functioning of the estuary and its associated ecosystem are determined to a large extent by mouth closure events. The Escoffier criteria for inlet stability indicate that the estuary is 'unstable' at best, or falls into the 'normally closed' category (Goodman, 1996). This means that any event (e.g. storm with high waves) causing the inlet cross sectional area to decrease is accompanied by a reduction in peak velocities which causes the cross-sectional are to decrease further, leading to inlet closure. The mouth is breached again when the river floods or it is breached artificially.

The Great Brak Estuary has a small town on its banks and a residential island located near the mouth. It is used intensively during holiday seasons for recreational purposes by tourists and, outside of these times, less intensively by local residents. The location of a dam, some 3 km above the head of tidal influence of the estuary has meant that the freshwater flows to the estuary are constrained with concomitant effects on the mouth. These include an increased incidence, and more sustained periods, of closure and necessitated artificial, mechanical breaching of the closed mouth (i) to alleviate the danger of flooding of low lying properties, (ii) to combat water quality deterioration, and (iii) to sustain the

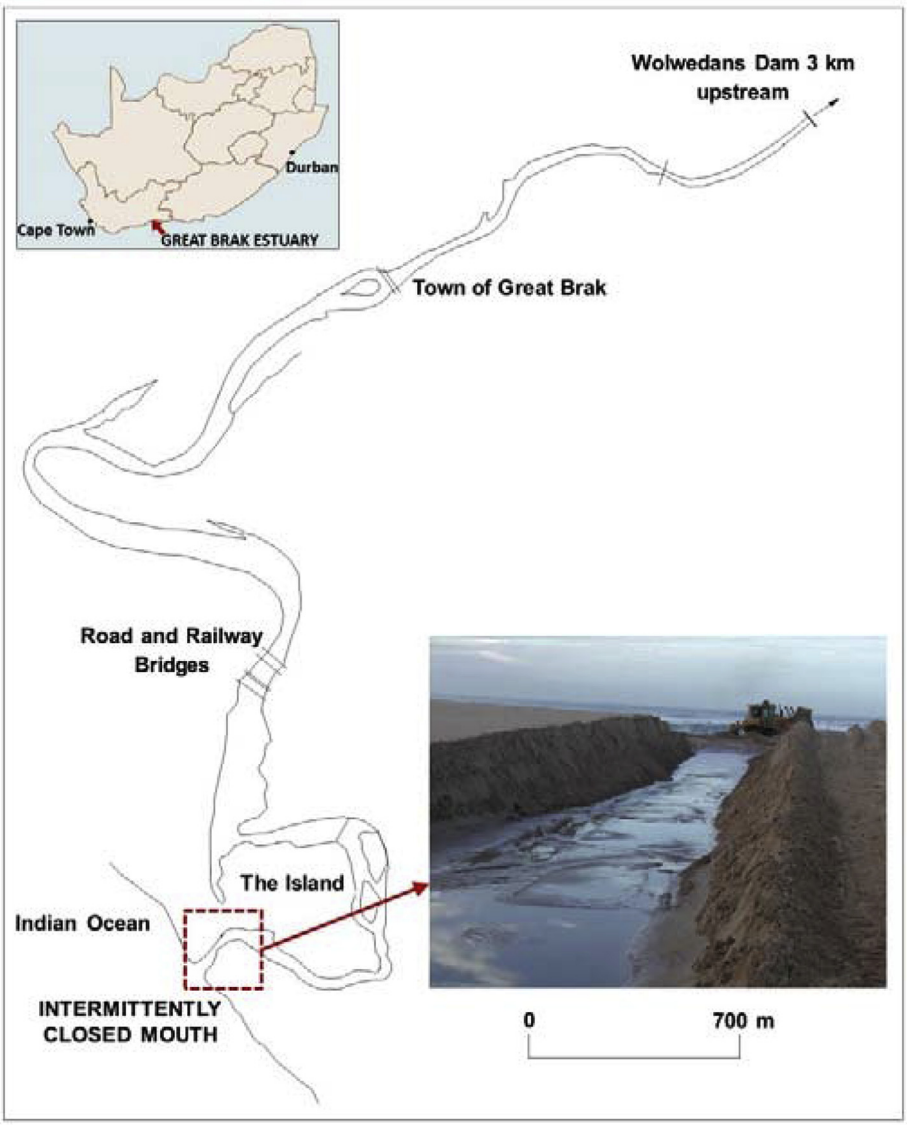

Fig. 2. The Great Brak Estuary, South Africa, is small (high tide area 0.6 km^2, tidal prism approximately 0.3 $\times$ 10^6 m^3) and its mouth is subject to intermittent closure. Artificial breaching of the mouth is sometimes required (photo insert: CSIR).

Please cite this article in press as: Slinger, J.H., Hydro-morphological modelling of small, wave-dominated estuaries, Estuarine, Coastal and Shelf Science (2016), http://dx.doi.org/10.1016/j.ecss.2016.10.038

estuarine ecosystem. A protocol for artificial breaching of the mouth is set out in the review of the management plan for the estuary (CSIR, 2003).

3.2. Calibration under low flow and flood conditions

Many of the data required for calibration are readily obtainable, such as tidal variations in the nearshore zone, significant wave heights in the bay, and water levels within the estuary, while other required data could be sourced from previous measurement campaigns (Slinger et al., 1994). These data were supplemented by observations of the breadth of the mouth, for instance, and consultation with local stakeholders and regional authorities, where necessary (Hermans et al., 2012; Slinger et al., 2012). Full details of the specification of the model for the Great Brak Estuary are listed in Tables A3 and A4 in the Appendix.

A stepwise calibration procedure is used in implementing the model on the Great Brak Estuary. This involves first calibrating the water volume sector, and then the sediment sector. Note that the simulation year begins on 1 October in all cases in accordance with the austral hydrological year. The bimodal annual rainfall pattern with enhanced evaporation over the hot summer months determines the variation in the net precipitation evaporation rate (Tables A3 and A4). No extreme rain events are simulated. Similarly in the initial calibration, the freshwater discharge is set to a low constant base flow of 0.1 $m^3\ s^{-1}$, representative of conditions without freshwater releases from the upstream Wolwedans Dam. The seepage rate is set to a small constant loss of water from the estuary (0.005 $m^3\ s^{-1}$), as this is the only available data. The tidal water levels are represented for calibration purposes by a simple cosine form with semi-diurnal and spring-neap features parametrized according to values from Table 2 of the Tide Tables published annually by the South African Navy Hydrographer (Tables A3). Next, the form of the estuary mouth is parametrized with values being assigned to the mouth width (18 m), and an initial value to the sill height (0,6 m to MSL). With these values in place, and the hypsometry of the estuary determined from surveys (Tables A4), the tidal flux is calibrated next. To achieve this, the velocity asymmetry function is first specified using direct measurements of flood and ebb velocities under low flow, open mouth conditions (cf. Lincoln and FitzGerald, 1988; Morris and Turner, 2010). In the absence of such measurements, water level variations indicating the duration and form of the flood and ebb tides can be used to estimate the velocity asymmetry function. The formulation chosen for the Great Brak case, given in Tables A4, generates the observed behavior of ebb tides characteristically lasting about 8 h and flood tides lasting a little in excess of 4 h. Finally, the initial sill height may need to be adjusted slightly so that the water level variations in the estuary reflect measured values.

Once the water volume sector is calibrated under low freshwater flow conditions, the sediment sector also needs to be calibrated under the same conditions. For the Great Brak Estuary, we know that the sill height at the mouth remains fairly constant over neap tides under low flow conditions and low waves (*pers. com.* P Huizinga). This information is used to determine whether the initial sill height value needs to be adjusted or not, and a cross-check is made with any concomitant effects on water level variations in the estuary. Once such refinements are completed, if necessary, the model can be calibrated for high flow conditions.

Detailed monitoring of a flood release on 29 and 30 November 1990 from the Wolwedans Dam and the associated flushing of the Great Brak Estuary is reported in Slinger et al. (1994). These data are used in calibrating the sediment sector of the model under high flow conditions. A comparison of the simulated and measured water levels in the estuary provides evidence that the evolution of the sill height is adequately modelled (Fig. 3). This agreement was achieved by reducing the volume of the bed used in the sediment formulation by 20% i.e. only considering 80% of the length of the mouth channel. When this adjustment was also tested under low flow conditions, and the model outcomes were robust to this change, it was adopted for all conditions. A final check was made by setting the wave stirring factor to an extreme value (wave height factor > 10), to check whether the estuary mouth would close under such an extreme condition of high sediment loads, as expected. When this occurred, and a further feature of the estuary was simulated under usual wave conditions, viz. a very slight modulation in the sill height at the mouth with spring and neap tides, the calibration of the model was deemed complete.

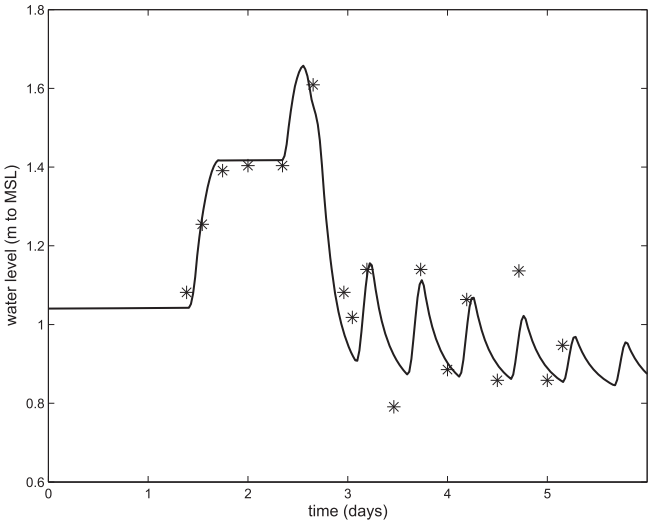

Fig. 3. Comparison between measured (*) and simulated water levels (—) in the Great Brak Estuary over 6 days from 28 November following a flood release and associated breaching of the mouth on 29, 30 November 1988.

3.3. Opening and closure of the estuary mouth under different freshwater flows

Prior to the construction of the Wolwedans Dam immediately upstream of the estuary, the average annual freshwater inflow to the estuary was 24 × 10^6 $m^3\ yr^{-1}$ with a bimodal seasonal distribution typical of the southeastern coast of South Africa (Tables A4). With this as the freshwater discharge rate, a policy of breaching between 1,6 and 1,85 m to MSL, and two high wave events in May and December (Table 1), a *Pre-dam* simulation was conducted for a period of 5 years. Results from the fourth year are presented in Fig. 4, beginning in October, the first month of the austral hydrological year. The representative nature of the simulation was affirmed by the interdisciplinary team of a multi-institutional collaborative research project (Slinger and Breen, 1995).

The mouth of the estuary closed and was breached artificially twice in a year. Following breaching of the mouth in December (month 3) and June (month 9), the sill height decreased to approximately 0,6 m to MSL and remained around this level until the next wave event transported sand into the mouth channel, choking and closing it. When the mouth was open, water levels in

Please cite this article in press as: Slinger, J.H., Hydro-morphological modelling of small, wave-dominated estuaries, Estuarine, Coastal and Shelf Science (2016), http://dx.doi.org/10.1016/j.ecss.2016.10.038

Table 1
Input conditions associated with the *Pre-dam*, *Post Dam with Releases*, and the *Post Dam with Base Flow* freshwater inflows to the Great Brak Estuary.

Differences in input conditions	*Pre-dam*	*Post Dam with Releases*	*Post Dam with Base Flow*
Annual volume	24×10^6 m^3 yr^{-1}	2×10^6 m^3 yr^{-1}	2×10^6 m^3 yr^{-1}
Distribution of freshwater inflow	Average annual volume multiplied by a bimodal seasonal distribution (rsm)	3 floods of 5×10^5 m^3 each on 29 November, 27 February, 15 September respectively, and a continuous base flow of 5×10^5 m^3 throughout the year	Average annual volume released as a base flow throughout the year
Height at which breaching occurs	Between 1,6 and 1,85 m to MSL	Between 1,6 and 1,85 m to MSL	Breaching is initiated at the same times as it proved necessary under the *Post Dam with Releases* simulation
Breaching rate	−0,2 m/hour for 2 h	−0,2 m/hour for 2 h	−0,2 m/hour for 3,5 h
Wave climate	High waves in late April/early May and Dec cause mouth closure.	High waves in November/Dec, February, late April/early May and mid-July cause mouth closure	High waves in November/Dec, February, late April/early May and mid-July cause mouth closure

Table 2
Response of the mouth of the Great Brak Estuary under different freshwater inflows to high wave events.

Indicative wave height factor (m)	Freshwater inflow (m^3.yr^{-1})		
	Natural 34×10^6	*Pre Dam* 24×10^6	*Post Dam* 2×10^6
3,82	open	open	open
3,97	open	open	closed
4,00	self-breaching	closed	closed
4,05	self-breaching	closed	closed
4,25	self-breaching	closed	closed
4,45	self-breaching	closed	closed
5,00	closed	closed	closed

the estuary varied from a minimum of 0,67 m to MSL over neap tides to a maximum of 0.94 m to MSL. Elevated low waters in the estuary during spring tides (>0,67 m to MSL) are a known feature of the Great Brak Estuary. The long duration, yet slow outflow of water through the constricted mouth during the ebb tides as the tidal cycle moves from the spring to the neap phase means that low water levels decline progressively further to a minimum at neap low tide before starting to increase again over each progressive ebb tide as the tidal cycle moves from neap to spring. This phenomenon of higher low water levels in the estuary during spring tide than during neap tide can be seen to be captured effectively in the simulation in Fig. 4.

When the mouth closed in December, tidal action ceased and water levels gradually increased to 1,63 m to MSL. The mouth was breached mechanically ten days after closure, reflecting the common practice of residents owing to concerns for recreation, inundation of property and vegetation health (CSIR, 1990). In contrast, when the mouth closed late in May, water levels rose to 1,82 m and remained near this level for 15 days before mechanical breaching was undertaken, as this is the low season for tourism and active estuarine vegetation growth. During both mouth closure events salinities in the estuary decreased, but rose again to maxima of 27 on the spring tides immediately following breaching.

Following dam construction, a high proportion of the freshwater inflow to the estuary derives from an average of three water releases to the estuary per annum. These are specified in the *Post Dam with Releases* simulation as flood water releases commencing on 29 November, 27 February and 15 September with volumes of 5×10^5 m^3, and a low base flow of the same volume spread evenly over the year (Table 1). In addition to the *Post Dam with Releases* simulation, deemed representative of the actual post dam situation by the interdisciplinary team of a multi-institutional collaborative research project (Slinger and Breen, 1995), a hypothetical situation in which the annual allocation of freshwater (2×10^6 m^3) is delivered to the estuary as continual low base flow, the *Post Dam with Base Flow* (Table 1), is also simulated.

In both the *Post Dam with Releases* and the *Post Dam with Base Flow* simulations (Figs. 5 and 6), the mouth of the estuary closed four times per year in November, February, late April and mid-July. The sill height attained values in excess of 1,6 m to MSL and remained at a high level until breached artificially. During the subsequent tidal phases, the sill height minima for both post dam simulations were close to 0,6 m to MSL. The water level in the estuary then exhibited very similar behavior to the *Pre Dam* simulation under open mouth conditions with water levels ranging between 0,67 m to MSL over neap tides to a maximum of 0,92 m to MSL over spring tides. However, marked differences occurred between the post dam simulations when the mouth was closed. Under the *Post Dam with Base Flow* situation, the water level in the estuary rose gradually after the mouth closed attaining an overall maximum of 1,37 m to MSL. The inflow to the system was insufficient to cause overflow or natural breaching. In contrast, under the *Post Dam with Releases* situation, the water level rose rapidly to 1,85 m to MSL, providing the infrequent inundation required for the health of elevated salt marsh, and effective breaching of the mouth occurred before vegetation dieback could occur. Under the *Post Dam with Releases* simulation, the volume averaged salinities in the estuary are anticipated to exceed 30, but decrease to about 10 three times a year when the flood releases occur and the mouth is still closed. Slightly lower volume averaged salinities would occur under open mouth periods for the *Post Dam with Base Flow* situation, but salinities are unlikely to decline below 15 even during the mouth closed periods.

The effects of reduced, and different, freshwater flows following the construction of the upstream dam on water levels within the Great Brak Estuary and the sill height at the mouth as simulated here, are reflected by the long term monitoring of the system. This has engendered confidence in the ability of the parametric model to capture behaviour characteristic of the Great Brak Estuary following the construction of the Wolwedans Dam. Unfortunately, the detailed measurement of sedimentary and water column changes during high flow events does not form an integral part of the ongoing low level monitoring programme, making further and more recent validation of the model results difficult.

Please cite this article in press as: Slinger, J.H., Hydro-morphological modelling of small, wave-dominated estuaries, Estuarine, Coastal and Shelf Science (2016), http://dx.doi.org/10.1016/j.ecss.2016.10.038

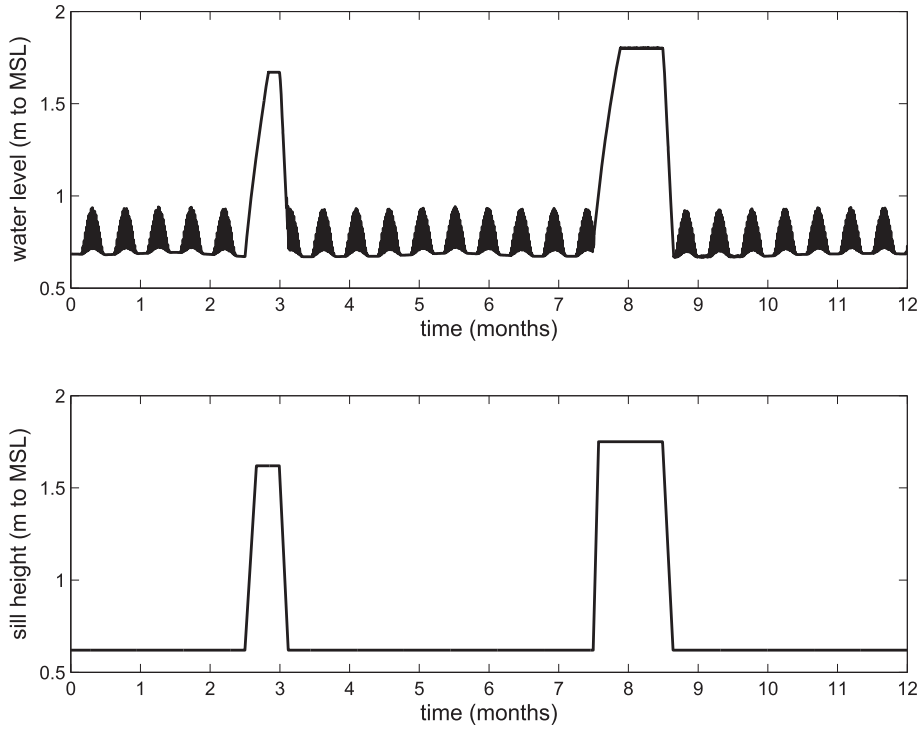

Fig. 4. Water level and sill height variations under the *Pre Dam* freshwater inflow regime, showing the closure and subsequent mechanical breaching of the mouth in months 3 and 4, and month 8 and 9, respectively.

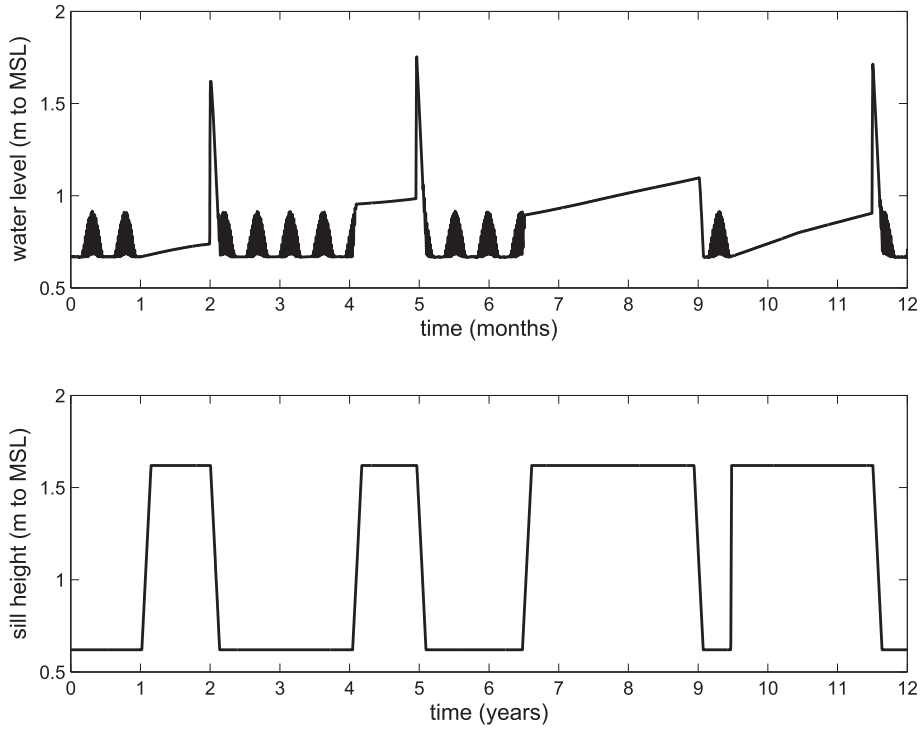

Fig. 5. Water level and sill height variations under the *Post Dam with Releases* freshwater inflow regime showing the closure and subsequent mechanical breaching of the mouth following flood releases (months 1–2, month 5, and months 10–12). No flood release occurred during the austral winter, instead the estuary received a continuous base flow, and mechanical breaching at the end of month 9.

Please cite this article in press as: Slinger, J.H., Hydro-morphological modelling of small, wave-dominated estuaries, Estuarine, Coastal and Shelf Science (2016), http://dx.doi.org/10.1016/j.ecss.2016.10.038

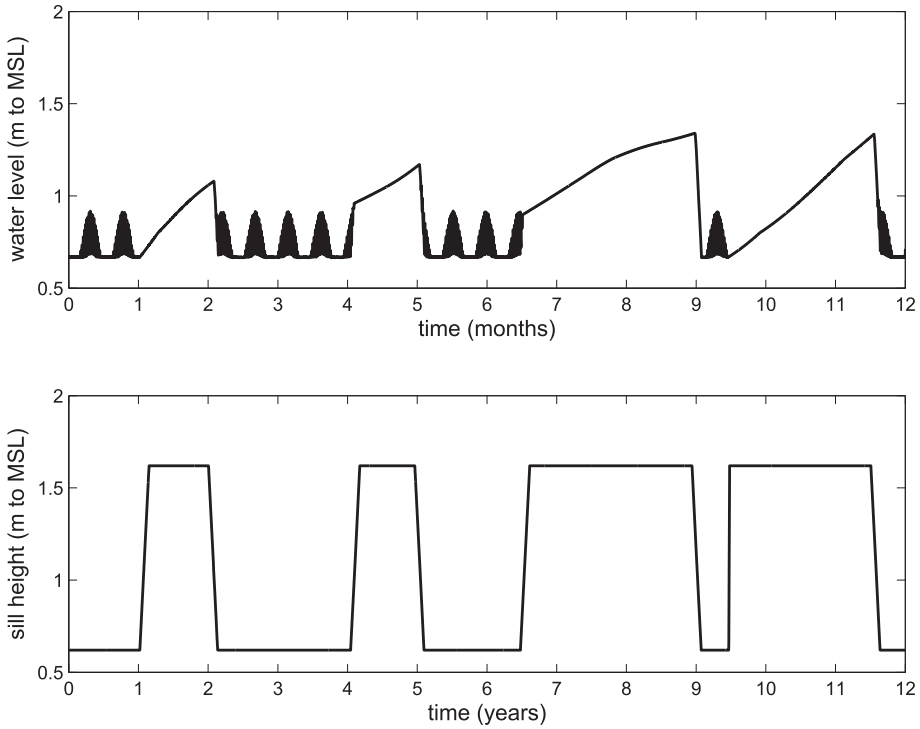

Fig. 6. Water level and sill height variations under the *Post Dam with Base Flow* freshwater inflow regime showing the closure and subsequent mechanical breaching of the mouth (months 1–2, month 5, months 7–9, and months 10–12). No flood releases occurred, instead the estuary received a continuous base flow, and mechanical breaching.

3.4. The influence of waves on mouth closure

The behavior of the Great Brak Estuary mouth and its sensitivity to closure from the enhanced sediment transported into the mouth channel under high wave conditions are intriguing. Accordingly, the parametric model application is extended to an exploration of the simulated response of the mouth to a number of high wave events of 3 day duration, commencing on 1 June, under three constant freshwater inflows typifying the *Natural* (pre-development), *Pre Dam* and *Post Dam* run-offs. No artificial breaching of the mouth is applied, instead the capacity of the estuary to restore an open mouth condition is explored. The behavior of the mouth in response to the wave events was classified as closed, open or self-breaching (Table 2). The mouth was considered closed if tidal exchange ceased entirely following the high wave event, but deemed open if tidal exchange still occurred immediately after the event albeit of reduced magnitude. The term self-breaching describes the situation in which tidal exchange ceases for some time after the wave event while the water level rises to the height of the berm and beyond and natural breaching of the mouth then occurs.

Only under freshwater flows characteristic of the natural, undeveloped catchment does the self-breaching capacity of the estuary manifest itself. This reflects historical observations of the Great Brak Estuary indicating that it closed infrequently in the past, and could breach naturally (CSIR, 1990). In contrast, the sensitivity of the mouth to closure is enhanced under freshwater inflows typical of the *Pre dam* and *Post dam* situations, with the transition between open and closed responses occurring in the range from 3,97 to 4,00 m and 3,82 to 4,00 m wave height factor, respectively. Of course, the different responses occasioned by such slight differences in the wave height factor are not entirely realistic – there are many factors playing a role in the actual response of an estuary mouth to storm events. This is simply an indication of the altered effect of wave events on the estuary mouth when all factors other than freshwater flow are held constant. The interpretation of these results is limited to (i) a confirmation that the sensitivity to closure by wave events is enhanced by anthropogenic reductions in freshwater inflows to the estuary, and (ii) that should higher wave events increase in frequency under climate change, more frequent and persistent closure of the estuary mouth may result.

4. Discussion

In recent years, research attention has turned to modelling the behavior of the inlet dynamics of small, wave-dominated estuaries (Duonga et al., 2015; Behrens et al., 2013, 2015). Prior to 2013, attention focused on characterizing the stability of tidal inlets using semi empirical criteria such as the Bruun Rule or the Escoffier coefficient (cf. Goodman, 1996), and studies focusing specifically on modelling the closure of such estuaries were limited to Slinger (1996) in South Africa and Ranasinghe et al. (1999) and Ranasinghe and Pattiaratchi (2003) in Australia. The renewed attention may have arisen from climate change studies, or increased anthropogenic pressures. After all, the non-linear dynamics of these tidal inlets present us with a tipping point in the response of small estuaries to altered storminess, sea level rise and increasing anthropogenic disturbance. Additionally, in a small number of cases, there is now sufficient data for use in validating models against measured behavior e.g. the Albufeira lagoon in Portugal, and the Russian river, California, and potentially the Narrabeen Lagoon, in Australia (Morris and Turner, 2010).

The parametric approach adopted in this paper means that even in the data poor situations that characterize small, wave-dominated estuaries, an understanding of the potential modes of

Please cite this article in press as: Slinger, J.H., Hydro-morphological modelling of small, wave-dominated estuaries, Estuarine, Coastal and Shelf Science (2016), http://dx.doi.org/10.1016/j.ecss.2016.10.038

behavior of these systems under altered physical forcing can be obtained. This holds promise, both for the continued use of this approach in exploring the response of such estuaries to climate change (cf. Duonga et al., 2015), and for the use in coastal management where the system understanding of stakeholders can be informed (cf. D'Hont et al., 2014). Indeed, the parametric approach to sedimentation in harbour channels is currently being extended (van Leeuwen, 2015) so as to provide a generic capability to make an initial assessment of the potential sedimentation in harbours, without having to undertake a detailed process-based model analysis from the outset.

The model developed and applied in this study can be located between the approaches of Rich and Keller (2013), and Behrens et al. (2013), as it uses studies on layer flow through constrictions and over sills to determine the maximum volume flux through the mouth. This insight regarding the manner in which the mouth channel acts to constrain tidal exchange is a strength of the Slinger model, and represents a more general manner for calculating the peak velocity used by Escoffier in his analysis (cf. Goodman, 1996) even for small estuaries where the depth of the mouth channel is small compared with the tidal range. Model outputs reveal that the elevation of the low water levels in the estuary during spring tide relative to neap tide – a typical feature of many small, wave-dominated estuaries – is reliably simulated. Moreover, freshwater inflows to the estuary are shown to be significant in determining the behaviour of the inlet mouth, a factor often ignored in studies on tidal inlets. Further, the study confirms that it is the balance between freshwater inflows and wave events that determines the opening or closure of the mouth of a particular estuary. This result was known for seasonal systems (Ranasinghe and Pattiaratchi, 2003), but also applies to irregular intermittently closed estuaries (Morris and Turner, 2010).

This paper has only addressed the water exchange and sediment component of small, wave-dominated estuaries. The full model of Slinger (1996) uses a parametric approach to provide an indicative simulation of the stratification state of an estuary and the percentage flushing of the estuary volume by tidal exchange. Simulation of these effects would allow for the inclusion of baroclinic effects on the volume flux through the mouth. Although, the full model has been implemented on the permanently open Kromme Estuary in South Africa (Slinger, 1996), and this version has been applied to the Slufter Estuary in the Netherlands (D'Hont, 2014), further testing is required to establish the limits of applicability of the approach. The applicability of the model to the Slufter under storm conditions when elevated water levels cause extensive flooding of the salt marshes, temporarily increasing the tidal prism to five times its normal volume and resulting in high flow velocities during ebb (Van der Vegt and Hoekstra, 2012), has not been established. Further, in the Great Brak, and the Kromme estuaries the alteration to the hypsometry of the estuary basin from the sediment not deposited in the mouth channel but transported into the estuary on the flood tide, was negligible. This is not always the case, and it would be interesting to determine when this effect could no longer be ignored and a hypsometric update step would be required.

5. Conclusion

The parametric approach to modelling the closure and opening of the inlet of small, wave-dominated estuaries has established that the pumping up, or elevation, of low water levels over spring tides relative to neap tides is primarily determined by the constraining effect of the mouth on tidal fluxes. Indeed, the closure of the mouth is strongly influenced by the freshwater entering the estuary, a factor often ignored in studies on tidal inlets. In addition, model results confirm that it is the balance between freshwater inflows and wave events that determines the opening or closure of the mouth of a particular estuary.

The ease of applicability of the approach has been demonstrated on an illustrative case study. More importantly, because of the low data demands, this approach now can be applied to more small estuaries with limited measured data. Of interest is the coherence between known responses, observations and model predictions. The range of applicability of the model, and similar parametric models, can then be established, and the understanding of the complementary nature of parametric modelling and process-based modelling can be deepened.

Acknowledgements

The support of the Multi-Actor systems research programme of the Faculty for Technology, Policy and Management, the Steuncampagne of the Faculty of Civil Engineering and Geosciences of the Delft University of Technology, and the CoCoChannel project funded by the Dutch National Science Foundation under grant number 850.13.043 are acknowledged. The original model was formulated and many of the data on the Great Brak estuary were measured while the author was employed at CSIR in Stellenbosch, South Africa. In addition, Floortje D'Hont, Dirk Jan Walstra and Susan Taljaard are acknowledged. The anonymous reviewers are thanked for their insightful and challenging comments.

Appendix 1. Model equations, list of symbols and parameter values

Table A1
Model equations

Water volume sector equations	Sediment sector equations
$h_L = twl - wl$	$d_{gr} = d[g(1-s)\nu^2]^{\frac{1}{3}}$
$ttflux = \frac{h_L}{L} H_s'(wl) V(twl, wl)$	$n = 1 - 0.56 log_{10} d_{gr} \quad for\ 1 \le d_{gr} \le 60$
$wl = H_s(x_1)$	$S_i = 0.23/\sqrt[2]{d_{gr}} + 1.14$
$a = bh$	$m = 9.66/d_{gr} + 1.34$
$h = \begin{cases} twl - x_2 & if\ twl > wl\ and\ twl > x_2 \\ wl - x_2 & if\ wl \ge twl\ and\ wl > x_2 \\ 0 & otherwise \end{cases}$	$c = 10^{(2.86 log_{10} d_{gr} - (log_{10} d_{gr})^2 - 3.53)}$
$G^2 = F_1^2 + F_2^2$	$u_* = \sqrt[2]{gh\lvert twl - wl\rvert / l}$
$F_i^2 = u_i / \sqrt[2]{g h_i}$	$\overline{u} = \lvert x_{14}\rvert / a\varepsilon$
$u_c = \sqrt[2]{gh}$	$S_{gr} = \frac{u_*^n}{\sqrt[2]{gd(s-1)}} \left(\frac{\overline{u}}{5.66 \frac{log_{10} 10h}{d}} \right)^{1-n}$
$c_f = \begin{cases} \frac{u_c a}{\lvert ttflux\rvert} & if\ u_c a < \lvert ttflux\rvert \\ 1 & otherwise \end{cases}$	$S_t = \begin{cases} c(S_{gr}/S_i - 1)^m & if\ S_{gr} > S_i \\ 0 & otherwise \end{cases}$
$x_{14} = ttflux.c_f$	$S_{vol} = S_t (d/h) (\overline{u}/u_*)^n$
$\frac{dx_1}{dt} = \sum_{i=1}^{4} x_{1i}$	$x_{21} = \begin{cases} S_{vol} x_{14} / bl(1-p_s) & if\ x_{14} < 0 \\ 0 & otherwise \end{cases}$
	$S_w = \begin{cases} c(\omega\beta S_{gr}/S_i - 1)^m & if\ \omega\beta S_{gr} > S_i \\ 0 & otherwise \end{cases}$
	$S_{mod} = S_w (d/h) (\overline{u}/u_*)^n$
	$x_{22} = \begin{cases} (S_{mod} - S_{vol}) x_{14} / bl(1-p_s) & if\ x_{14} > 0 \\ 0 & otherwise \end{cases}$
	$\frac{dx_2}{dt} = \sum_{i=1}^{3} x_{2i}$

Please cite this article in press as: Slinger, J.H., Hydro-morphological modelling of small, wave-dominated estuaries, Estuarine, Coastal and Shelf Science (2016), http://dx.doi.org/10.1016/j.ecss.2016.10.038

Table A2
List of symbols

Water volume sector symbols	Sediment sector symbols
x_1 = *water volume* (m^3)	x_2 = *sill height at the mouth* (*m to MSL*)
x_{11} = *freshwater inflow rate* (m^3/yr)	x_{21} = *sill accretion rate* (m/yr)
x_{12} = *net precipitation evaporation rate* (m^3/yr)	x_{22} = *sill erosion rate* (m/yr)
x_{13} = *seepage rate* (m^3/yr)	x_{22} = *sill breaching rate* (m/yr)
x_{14} = *tidal flow through the mouth* (m^3/yr)	*length of the mouth* (m)
wl = *water level relative to mean sea level* (*m to MSL*)	d = *grain diameter* (m)
twl = *tidal water level relative to mean sea level* (m)	d_* = *dimensionless grain diameter*
$ttflux$ = *target tidal flux* (m^3)	ν = *kinematic viscosity of fluidood* (m^2/s)
h_L = *hydraulic head* (m)	s = *mass density of sand relative to fluid* (*dimensionless*)
L = *characteristic length of the estuary* (m)	ε = *conversion constant* ($3{,}1536 \times 10^7$ s/yr)
$H'_S(wl)$ = *hypsometric function of water level* (m^3)	S_{gr} = *particle mobility* (*dimensionless*)
$H_S(x_1)$ = *hypsometric function of water level* (m)	S_i = *initial motion parameter, critical threshold* (*dimensionless*)
$V(twl,wl)$ = *velocity function of tidal water level, water level* (*dimensionless*)	n = *transition exponent* (*dimensionless*)
x_2 = *sill height at the mouth* (*m to MSL*)	m = *transition exponent in sediment transport formula* (*dimensionless*)
a = *cross sectional area in the mouth* (m^2)	c = *coefficient in sediment transport formula* (*dimensionless*)
b = *breadth of the mouth* (m)	u_* = *shear stress* (m/s)
h = *effective depth of flow in the mouth* (m)	$\overline{u}$ = *mean flow* (m/s)
G = *two layer composite Froude number*	S_t = *sediment transport capacity* (*dimensionless*)
F_i = *layer densimetric Froude number*	S_{vol} = *volumetric sediment transport rate* (m^3sand/m^3water)
u_i = *layer flow velocity* (m/s)	p_s = *porosity of the sandy bed*
g = *gravitational acceleration* (m/s^2)	β = *topograpic factor*(*dimensionless*)
g' = *reduced gravitational acceleration* (m/s^2)	ω = *wave stirring factor*(*dimensionless*)
u_c = *critical layer flow velocity* (m/s)	S_w = *volumetric sedimenttransport rate* (m^3sand/m^3water)
c_f = *control factor* (*dimensionless*)	S_{mod} = *enhanced volumetric sediment transport rate* (m^3/m^3)

Table A3
Parameter values used (at the start) in the simulation.

Parameter and symbol	Value and units for the Great Brak case	Explanation
Mean sea level (MSL)	0,24 m	The formula used to calculate the tidal water level: $twl = MSL + \alpha_1 \cos\left(\frac{2\pi t}{T_1}\right)\left(1 + \alpha_2 \cos\left(\frac{2\pi t}{T_2}\right)\right)$
Semi-diurnal tidal amplitude (α_1)	0,58 m	
Semi-diurnal time scale (T_1)		
Semi-diurnal time scale (T_1)		
Spring-neap tidal amplitude (α_2)	0,509 m	
Spring-neap time scale (T_2)		
Net rainfall evaporation	0,5056−1315 m/yr	The formula used to calculate the net rainfall evaporation: $x_{12} = 0{,}5056$ SA *rsm* − 1.315 SA *esm* The rainfall seasonal multiplier (*rsm*) and the evaporation seasonal multiplier (*esm*) are specified in Tables A4, and the surface area (*SA*) is specifies below.
Seepage rate (x_{13})	−157680 m^3/yr	Set at a constant value for the Great Brak Estuary to represent the estuarine water seeping through the permanent sand berm that separates the estuary from the sea, whether the mouth is closed or open.
Surface area (*SA*)	470,500 m^2	Average surface area of the estuary as first reported in Morant (1983). The surface area is included in the formula for the Net rainfall evaporation rate
Characteristic length parameter (L)	250 m	Characteristic length parameter. Determined as the distance from the mouth to the point in the estuary basin where water level variations are most representative of the estuary dynamics. Because the Great Brak has a wide basin with deeper parts near the sea and narrow upper reaches with only isolated deep pools, the characteristic length of the estuary lies at the highway bridges near the mouth (Fig. 2).
Breadth of the mouth (b)	18 m	Breadth of the estuary mouth, measured at the widest point.
Initial sill height	0,6 m to MSL	Usually set to the sill height under conditions of low freshwater flow and low waves for which the mouth remains open.
Grain size (d_{50})	$0{,}45 \times 10^{-3}$ m	Measured grain size as first reported in Morant (1983)
Porosity (p_s)	0,4	Volumetric porosity of sand is 40%
Length of the mouth (l)	10 m	Length of the mouth channel – best estimated during flood flows, or estimated as the length of the channel that needs to be dug to breach the mouth artificially, as in the case of the Great Brak Estary.
Shoreface topography factor (β)	1,0	A shoreface topography factor of less than unity, indicates sheltering of the nearshore zone immediately in front of the estuary mouth from wave action e.g. by a headland or groyne. A shoreface topography factor of greater than unity indicates increased exposure of the estuary mouth to wave action. A value of unity is assigned to the Great Brak as no unusual shoreface topography effects are present.
Wave stirring factor (ω)	1,0	The wave stirring factor is exogenously specified to represent the effects of increased wave heights in stirring sediment up into suspension. It comprises the seasonal wave climate derived from wave measurements multiplied by a wave height factor (nearshore significant wave height) to represent the effects of storms at times.

Please cite this article in press as: Slinger, J.H., Hydro-morphological modelling of small, wave-dominated estuaries, Estuarine, Coastal and Shelf Science (2016), http://dx.doi.org/10.1016/j.ecss.2016.10.038

Table A4
Estuary hypsometry, velocity asymmetry, and the rainfall, evaporation and wave climate functions

Water volume (m^3)	Water level (m to MSL)	Hydraulic head (*twl-wl/l*)	Velocity asymmetry function	Time (from 1 October in months)	Rainfall seasonal multiplier	Evaporation seasonal multiplier	Wave climate function
1,0	−1	−0,006	1,05	0.0	1.233	0.825	1.139
5,0	−0,2	−0,004	1,05	0.5	1.134	0.943	1.085
15,000,0	0.0	−0,002	1,00	1.5	1.510	1.375	0.950
33,000,0	0.2	−0,001	0,90	2.5	0.871	1.768	0.950
92,200,0	0.4	0,000	0,85	3.5	0.862	1.571	1.085
245,300,0	0.8	0,001	0,90	4.5	0.931	1.375	1.085
454,000,0	1.2	0,002	1,00	5.5	1.440	1.178	1.139
706,200,0	1.6	0,003	3,15	6.5	0.912	0.884	1.194
1,005,800,0	2.0	0,004	3,80	7.5	0.912	0.638	1.356
1,354,500,0	2.4	0,006	4,00	8.5	0.489	0.540	2.007
				9.5	0.686	9.432	1.628
				10.5	1.172	0.589	1.356
				11.5	1.332	0.707	1.248
				12.0	1.233	0.825	1.139

References

Ackers, P., White, W.R., 1975. Sediment transport, new approach and analysis. J. Hydraul. Div 2041–2060. ASCE 99, No HY 11.

Anthony, E.J., Oyédé, L.M., Lang, J., 2002. Sedimentation in a fluvially infilling, barrier-bound estuary on a wave-dominated, microtidal coast: the Ouémé River estuary, Benin, west Africa. Sedimentology 49, 1095–1112. http://dx.doi.org/10.1046/j.1365-3091.2002.00491.x.

Armi, L., Farmer, D.M., 1986. Maximal two-layer exchange through a contraction with barotropic net flow. J. Fluid Mech. 164, 27–51.

Aubrey, D.G., Speer, P.E., 1985. A study of non-linear tidal propagation in shallow inlet/estuarine systems. Part I: Observations. Estuar. Coast. Shelf Sci. 21, 185–205.

Behrens, D.K., Bombardelli, F.A., Largier, J.L., Twohy, E., 2013. Episodic closure of the tidal inlet at the mouth of the Russian River — a small bar-built estuary in California. Geomorphology 189, 66–80.

Behrens, D.K., Brennan, M., Battalio, P.E., 2015. A quantified conceptual model of inlet morphology and associated lagoon hydrology. Shore Beach 83 (3), 33–42.

Cooper, J.A.G., 2001. Geomorphological variability among microtidal estuaries from the wave-dominated South African coast. Geomorphology 40, 99–122.

CSIR, 1990. Great Brak River Environmental Study with Reference to a Management Plan for the Wolwedans Dam. CSIR Report EMA-C9036, Stellenbosch, South Africa.

CSIR, 1991. Sedimentation in the Kromme Estuary: Data Report. CSIR Report EMA-D9108, Stelenbosch, Sout Africa.

CSIR, 2003. Great Brak Estuary Management Programme Review Report. CSIR Report ENV–S–C–2003-092, Stellenbosch, South Africa, p. 18. Retrieved from. https://www.dwaf.gov.za/wma/wcape/gouritz/greatbrak/great%20brak%20estuary%20management%20review%20reports%202003/01_Great_Brak_Estuary_Management_Programme_Review_Report-March-2003.pdf.

Dalrymple, R.W., Zaitlin, B.A., Boyd, R., 1992. Estuarine facies models; conceptual basis and stratigraphic implications. J. Sediment. Petrol. 62, 1130–1146.

Day, J.H., 1981. Estuarine Ecology with Particular Reference to Southern Africa. Balkema, Cape Town, p. 411.

Duonga, T.M., Ranasinghe, R., Walstra, D.J.R., Roelvink, D., 2015. Assessing Climate Change Impacts on the Stability of Small Tidal Inlet Systems: Why and How? Earth Science Reviews. http://www.sciencedirect.com/science/article/pii/S0012825215300775.

D'Hont, F.M., 2014. Does Deepening Understanding of Social-ecological Systems Make Sense? A Partial Success Story from the Slufter, Texel. MSc thesis. Delft University of Technology Delft, Netherlands.

D'Hont, F., Slinger, J.H., Goessen, P., 2014. A knowledge intervention to explore stakeholders' understanding of a dynamic coastal nature reserve. In: 32nd International Conference of the System Dynamics Society. System Dynamics Society.

Elias, E., 2006. Morphodynamics of Texel Inlet. Phd dissertation. Delft University of Technology, Delft, Netherlands.

Eysink, W., Vermaas, H., 1983. Computational Methods to Estimate the Sedimentation in Dredged Channels and Harbour Basins in Estuarine Environments, 1st International Conference on Coastal and Port Engineering in Developing Countries.

Farmer, D.M., Armi, L., 1986. Maxima two-layer exchange over a sill and through the combination of a sill and contraction with barotropic flow. J. Fluid Mech. 164, 53–76.

Forrester, J.W., 1961. Industrial Dynamics. Pegasus Communications, Waltham, MA.

Forrester, J.W., 2007. System dynamics—a personal view of the first fifty years. Syst. Dyn. Rev. 23 (2–3), 345–358.

Fortunatoa, A.B., Nahona, A., Dodeta, G., Piresc, A.R., Freitasc, M.C., Bruneaud, N., Azevedoa, A., Bertinb, X., Benevidesa, P., Andradec, C., Oliveiraa, A., 2014. Morphological evolution of an ephemeral tidal inlet from opening to closure: the Albufeira inlet, Portugal. Cont. Shelf Res. 73 (1), 49–63.

Goodman, P., 1996. Predicting the stability of tidal inlets for wetland and estuary management. J. Coast. Res. 23, 83–101.

Green, G., 1837. On the motion of waves in a variable canal of small depth and width. Trans. Camb. Philosophical Soc. 6, 457–462.

Héquettea, A., Hemdaneb, Y., Anthony, E.J., 2008. Sediment transport under wave and current combined flows on a tide-dominated shoreface, northern coast of France. Mar. Geol. 249 (3–4), 226–242.

Hermans, L.M., Slinger, J.H., Cunningham, S.W., 2012. The use of monitoring information in policy-oriented learning: insights from two cases in coastal management. Environ. Sci. &Policy 29, 24–36. http://dx.doi.org/10.1016/j.envsci.2013.02.001.

Ippen, A.T., Harleman, D.R.F., 1966. Tidal dynamics in estuaries. In: Ippen, A.T. (Ed.), Estuary and Coastline Hydrodynamics. McGraw-Hill, New York, pp. 493–545.

Jacobs, D.K., Stein, E.D., Longcore, T., 2011. Classification of California Estuaries Based on Natural Closure Patterns: Templates for Restoration and Management (Revised) Technical Report 619a. Southern California Coastal Water Research Project, p. 67. Retrieved from. http://www.urbanwildlands.org/Resources/619.a_EstuarineClassificationRestorationDesign.pdf.

Largier, J.L., Slinger, J.H., 1991. Circulation in highly stratified southern African estuaries. South Afr. J. Aquat. Sci. 17 (1/2), 103–115.

Lesser, G.R., Roelvink, J.A., van Kester, J.A.T.M., Stelling, G.S., 2004. Development and validation of a three dimensional morphological model. J. Coast. Eng. 51, 883–915.

Lincoln, J., FitzGerald, D., 1988. Tidal distortions and flood dominance at five small tidal inlets in southern Maine. Mar. Geol. 82, 133–148.

McLaughlin, K., Sutula, M., Busse, L., Anderson, S., Crooks, J., Dagit, R., Gibson, D., Johnston, K., Stratton, L., 2013. A regional survey of the extent and magnitude of eutrophication in mediterranean estuaries of Southern California, USA. Estuaries Coasts 37 (2), 259–278.

Mendoza, E., Castillo-Rivera, M., Zárate-Hernández, R., Ortiz-Burgos, S., 2009. Seasonal variations in the diversity, abundance, and composition of species in an estuarine fish community in the Tropical Eastern Pacific, Mexico. Icthyol. Res. 56 (4), 330–339. http://dx.doi.org/10.1007/s10228-009-0102-5.

Morant, P.D., 1983. Estuaries of the Cape: Part II. Synopses of available information on individual systems. In: Heydorn, A.E.F., Grindley, J.R. (Eds.), Report 20. Groot Brak (CMS 3). CSIR Research Report 419, p. 51. Stellenbosch, South Africa.

Morris, B.D., Turner, I.L., 2010. Morphodynamics of intermittently open–closed coastal lagoon entrances: new insights and a conceptual model. Mar. Geol. 271, 55–66.

Nadaoka, K., Ueno, S., Igarashi, T., 1988. Sediment suspension due to large scale eddies in the surf zone. In: Proceedings of the 21st Coastal Engineering Conference, pp. 1646–1660.

Nakato, T., 1990. Tests of selected sediment-transport formulas. J. Hydraul. Eng. 3 (362), 362–379. http://dx.doi.org/10.1061/(ASCE)0733-9429(1990)116.

Officer, C.B., 1976. Physical Oceanography of Estuaries (And Associated Coastal Waters). John Wiley and Sons, New York, p. 465.

Ranasinghe, R., Pattiaratchi, C., 2003. The seasonal closure of tidal inlets: causes and effects. Coast. Eng. 45 (4), 601–627.

Ranasinghe, R., Pattiaratchi, C., Masselink, G., 1999. A morphodynamic model to simulate the seasonal closure of tidal inlets. Coast. Eng. 37, 1–36.

Rich, A., Keller, E.A., 2013. A hydrologic and geomorphic model of estuary breaching and closure. Geomorphology 191, 64–74.

Roy, P.S., Williams, R.J., Jones, A.R., Yassini, R., Gibbs, P.J., Coates, B., West, R.J., Scanes, P.R., Hudson, J.P., Nichol, S., 2001. Structure and function of south-east Australian estuaries. Estuar. Coast. Shelf Sci. 53, 351–384.

Schumann, E.H., Largier, J.L., Slinger, J.H., 1999. Estuarine hydrodynamics. In: Allanson, Baird, D. (Eds.), Estuaries of South Africa. Cambridge University Press,

Cambridge, United Kingdom, pp. 27–52 (Chapter 3).
Slinger, J.H., 1996. Modelling the Physical Dynamics of Estuaries for Management Purposes. PhD thesis. University of KwaZulu-Natal, Pietermaritzburg, South Africa, p. 205.
Slinger, J.H., Breen, C.M., 1995. Integrated research into estuarine management. Water Sci. Technol. 32 (5–6), 79–86. http://www.iwaponline.com/wst/03205/wst032050079.htm.
Slinger, J.H., Taljaard, S., Largier, J.L., 1994. Changes in estuarine water quality in response to a freshwater flow event. In: Dyer, K.R., Orth, R.J. (Eds.), Changes in Fluxes in Estuaries. Olsen & Olsen, Denmark, pp. 51–56. ECSA22/ERF Symposium.
Slinger, J.H., Huizinga, P., Taljaard, S., Van Niekerk, L., Enserink, B., 2005. From impact assessment to effective management plans: learning from the Great Brak Estuary in South Africa. Impact Assess. Proj. Apprais. 23 (3), 197–204.
Slinger, J., Linnane, S., Taljaard, S., Palmer, C., Hermans, L., Cunningham, S., van Niekerk, L., van den Hurk, M., Greter, S., Clifford-Holmes, J., 2012. From policy to practice: enhancing implementation of water policies for sustainable development. The story of the Great Brak. water Soc. 18.
Speer, P.E., Aubrey, D.G., 1985. A study of non-linear tidal propagation in shallow inlet/estuarine systems. Part II: Theory. Estuar. Coast. Shelf Sci. 21, 207–224.
Stommel, H., Farmer, H.G., 1953. Control of salinity in an estuary by a transition. J. Mar. Res. 12, 13–20.
Taljaard, S., van Niekerk, L., Joubert, W., 2009. Extension of a qualitative model on nutrient cycling and transformation to include microtidal estuaries on wave-dominated coasts: Southern hemisphere perspective. Estuar. Coast. Shelf Sci. 85 (3), 407–421. http://dx.doi.org/10.1016/j.ecss.2009.09.006.
Tung, T. T., Walstra, D. J. R., van de Graaff, J., Stive, M.J.F. (2009). Morphological modeling of tidal inlet migration and closure. Journal of Coastal Research Special Issue No. 56. Proceedings of the 10th International Coastal Symposium ICS 2009, Vol. II:1080–1084.
van Leeuwen, Y.B., 2015. Port and Channel Sedimentation. A Hybrid Model for Rapid Assessments. MSc thesis. Delft University of Technology, Delft, Netherlands.
van Rijn, L., 2007. Unified view of sediment transport by currents and waves. II: suspended transport. J. Hydraul. Eng. 133 (6), 668–689. http://dx.doi.org/10.1061/(ASCE)0733-9429(2007)133:6(668).
van Rijn, L.C., 2013. Basics of Channel Deposition/siltation. AquaPublications, The Netherlands. www.aquapublications.nl.
Van der Vegt, Hoekstra, 2012. Morphodynamics of a storm-dominated, shallow tidal inlet: the Slufter, The Netherlands. Neth. J. Geosci. — Geol. en Mijnbouw 91 (3), 325–339.
Wijnberg, K., Mulder, J., Slinger, J., van der Wegen, M., van der Spek, A., 2015. Challenges in Developing 'Building-with-nature' Solutions Near Tidal Inlet. Presented at *Coastal Sediments' 15 Understanding and working with nature*, 1–15 May 2015, San Diego, CA, USA.

Please cite this article in press as: Slinger, J.H., Hydro-morphological modelling of small, wave-dominated estuaries, Estuarine, Coastal and Shelf Science (2016), http://dx.doi.org/10.1016/j.ecss.2016.10.038